A NUMERICAL STUDY OF IMPULSIVELY STARTED EXTERNAL CONVECTION AT MICROSCALE

K. Ramadan *

Department of Mechanical Engineering
Mu'tah University
P. O. Box 7, Karak 61710, Jordan

ABSTRACT

Impulsively started external convection at microscale level is studied numerically in both planar and axisymmetric geometries. Using similarity transformation, the resulting coupled partial and non-linear ordinary differential equations are simultaneously solved by finite differences together with a well established ordinary differential equation solver, over a range of problem parameters. Rarefaction effects within the slip flow regime on the thermal boundary layer response, heat transfer rate and transition time when system experiences sudden changes in surface temperature are analyzed, and a comparison between sudden surface cooling and heating is presented. The results show that the thermal boundary layer thickness, heat transfer rate and the transition time is considerably influenced by the degree of rarefaction. The transition time tends to be less sensitive with increasing rarefaction. The velocity slip and temperature jump factors are found to have opposite effects on the transition time and the heat transfer rate, with the velocity slip factor having the most profound influence on these parameters.

Keywords: Microscale, Rarefaction, Slip flow, Velocity slip, Temperature jump, Transient convection.

1. INTRODUCTION

The study of fluid flow and heat transfer at the microscale level is a research area of continuous interest with many practical applications, such as microelectromechanical systems [1] and micro-air vehicles [2,3]. Fluid flow and heat transfer at the micrscale level is dominated by surface interactions, such as slip effects and thermal creep, as well as viscous dissipation and compressibility effects [1]. As the Knudsen number (defined as the mean free path of the fluid molecules to a characteristic length of the flow) increases, the departure from the continuum postulate increases, leading to momentum and thermal non-equilibrium conditions at the solid-fluid interface. In the slip flow regime, where the Knudsen number is in the range $0 \le Kn \le 0.1$, the non-equilibrium conditions at the solid-fluid interface are modeled as velocity slip and temperature jump conditions, whilst the continuum postulate is assumed to be valid [1], allowing the use of the continuum mechanics equations. The velocity slip condition relates the slip in the fluid velocity at the surface to the velocity gradient normal to the surface as well as the temperature gradient in the tangential direction to the surface, while the temperature jump relates the jump in temperature at the surface to the temperature gradient normal to the surface.

Slip effect on the hydrodynamic boundary layer was studied in [4] using a first order velocity-slip condition for a laminar flow over a stationary flat plate. The wall shear stress and the hydrodynamic boundary layer thickness were shown to decrease continuously with increasing the velocity slip. The same problem was revisited in [5] incorporating the slip condition in three different ways. The wall shear stress, skin friction coefficient, drag coefficient, boundary layer thickness, displacement thickness and momentum thickness were all found to decrease with increasing the velocity slip. Stagnation-point heat transfer near the continuum limit was studied in [6] with coupling between the velocity slip and temperature jump conditions. The results presented therein indicated a decrease in the heat transfer rate as the slip parameter increases. The study in [4] was further extended by the same authors to include the heat transfer problem [7]. The loss of self-similarity with the slip conditions was treated in a ways that the boundary layer equations are transformed into partial differential equations with the slip factor as an additional independent variable in the transformed equations. For an isothermal surface and first order slip conditions, the heat transfer rate was found to increase with increasing the velocity slip and no temperature jump. With temperature jump, the heat transfer rate was found to decrease below the no-slip values. The surprising result in [7] was that the friction and heat transfer rate have peak values at some finite non-zero slip parameter, so that the heat transfer decreases in highly rarefied flows and increases under moderately

* Corresponding author (rkhalid@mutah.edu.jo)

DOI : 10.1017/jmech.2014.33
Copyright © 2014 The Society of Theoretical and Applied Mechanics, R.O.C.
https://doi.org/10.1017/jmech.2014.33 Published online by Cambridge University Press

rarefied conditions with increasing the slip factor. Slip boundary conditions were also implemented in [8] to study the momentum and heat transfer for a laminar flow over a wedge using the same formulation as in [7]. The results show that the effect of slip conditions is to decrease the skin friction coefficient, boundary layer thickness, displacement thickness and momentum thickness. The heat transfer was found to increase for slightly rarefied flows, then decrease as the Knudsen number increases. Laminar boundary layer slip flow over a flat plate exposed to a constant surface heat flux was studied in [9]. The coupling between the momentum and energy equations at the solid –fluid interface due to the variation of the plate surface temperature was ignored. The results presented therein indicated an increase in the slip velocity and a decrease in the wall shear stress as the slip parameter increases, confirming the conclusions reached in [4]. The results also showed that an increase in the Prandtl number and/or the slip parameter results in a decrease in the surface temperature.

The studies in [4-9] were performed under steady state conditions to investigate slip effects on fluid flow and heat transfer. Attention has been directed towards exploring slip effects on transient flow and heat transfer, and some studies appeared in literature that analyze slip flow with unsteady state conditions. However, most of these studies focus on internal (microchannel) flow geometries [10-14], while transient external slip flow has received less attention. One of the early investigations of slip effects on transient external flow, was that in [15] where the Rayleigh problem was revisited with slip effects. Unsteady mixed convection on a stretching surface was studied in [16], and it was shown that the heat transfer rate decreases with the velocity slip parameter and increases with the unsteadiness parameter. This study was further extended [17] to investigate unsteady stagnation point flow on a stretching sheet with slip effects, and it was found that the heat transfer rate and skin friction change significantly due velocity and thermal slip parameters. In order to derive similarity solutions in [16,17], many restrictions were imposed on the flow field, velocity-slip and temperature-jump factors, surface stretching rate and the surface temperature. For example, the far-field fluid velocity and the surface stretching rate were taken to change in the same functional form. Furthermore, the velocity-slip and temperature-jump parameters were assumed to vary in time and in the same functional form that is related in some way to the surface stretching rate and the far-field fluid velocity.

The conclusion that may be drawn from this survey is that transient convection with rarefaction effects has seen only little coverage in the literature. Moreover, although the momentum and thermal accommodation coefficients are related, they are generally not equal [18,19]. Therefore the motivation is to investigate the individual effects of these momentum and thermal discontinuities on heat transfer rate, thermal boundary layer response and the transition time when the surface is exposed to an impulsive temperature change. This work presents a numerical study of transient external forced convection with velocity-slip and temperature-jump conditions in both two-dimensional and axisymmetric stagnation point flow configurations. A comparison between system response to surface sudden cooling and heating is also presented for both plane two-dimensional and axisymmeric flow configurations.

2. PROBLEM FORMULATION

The problem geometry of stagnation point flow is shown in Fig. 1, in addition to typical velocity and temperature profiles with velocity slip and temperature jump at the surface. For an incompressible, laminar flow with constant fluid properties and negligible viscous dissipation effects, the governing equations in two-dimensional and axisymmetric settings are given as [20,21]:

$$\frac{\partial}{\partial x}(x^{n-2}u)+\frac{\partial}{\partial y}(x^{n-2}\upsilon)=0 \tag{1}$$

$$u\frac{\partial u}{\partial x}+\upsilon\frac{\partial u}{\partial y}=-\frac{1}{\rho}\frac{\partial P}{\partial x}+\nu\left[\frac{\partial^2 u}{\partial x^2}+\frac{\partial}{\partial x}\left(\frac{u^{n-2}}{x^{n-2}}\right)+\frac{\partial^2 u}{\partial y^2}\right] \tag{2}$$

$$u\frac{\partial \upsilon}{\partial x}+\upsilon\frac{\partial \upsilon}{\partial y}=-\frac{1}{\rho}\frac{\partial P}{\partial y}+\nu\left[\frac{1}{x^{n-2}}\frac{\partial}{\partial x}\left(x^{n-2}\frac{\partial \upsilon}{\partial x}\right)+\frac{\partial^2 \upsilon}{\partial y^2}\right] \tag{3}$$

$$\frac{\partial T}{\partial t}+u\frac{\partial T}{\partial x}+\upsilon\frac{\partial T}{\partial y}=\alpha\left[\frac{1}{x^{n-2}}\frac{\partial}{\partial x}\left(x^{n-2}\frac{\partial T}{\partial x}\right)+\frac{\partial^2 T}{\partial y^2}\right] \tag{4}$$

where u, υ are respectively the velocity components in the x- and y- directions, and the index n is:

$$n=\begin{cases}2, & \text{for two-dimensional flow}\\ 3, & \text{for axisymmetric flow}\end{cases} \tag{5}$$

The physical situation of the problem is as follows: A far-field fluid at a constant temperature of T_∞ and velocity U impinges on as surface that is initially ($t < 0$) at a constant temperature T_{si}. The surface temperature is then impulsively changed (at $t = 0$) to a temperature T_{sf} that remains constant. Due to this sudden temperature change the system undergoes a transition process from the initial steady state, until the final steady state is reached. The thermal response of the system during the transition period from the initial- to the final steady state is theoretically studied in the presence of velocity-slip and temperature-jump conditions at the surface.

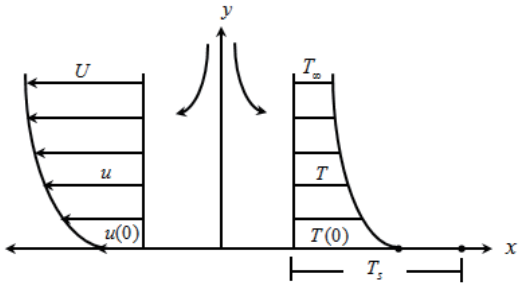


Fig. 1 Typical velocity and temperature profiles in stagnation point flow with velocity slip and temperature jump conditions

https://doi.org/10.1017/jmech.2014.33 Published online by Cambridge University Press

The boundary conditions for the velocity field are given as follows: the first order slip velocity at the stationary surface is given as [1,8]:

$$u(x,\ y=0)=\frac{2-\sigma_V}{\sigma_V}\lambda\frac{\partial u}{\partial y}(x,\ y=0)+\frac{3}{4}\frac{\mu}{\rho T}\frac{\partial T}{\partial x}(x,\ y=0) \tag{6}$$

where λ is the fluid mean-free-path, and σ_V is the momentum accommodation coefficient defined as the fraction of molecules incident on a surface that is reflected diffusively, hence σ_V is equal to zero for specular reflection and is equal to 1 for diffuse reflection and is dependent upon the fluid and solid properties as well as on the surface finish. Practically its experimental value is in the range between 0.2 for exceptionally smooth surfaces and 0.8 for most practical surfaces [1].

The surface is assumed impermeable, hence:

$$\upsilon(x,\ y=0)=0 \tag{7}$$

And the far-field fluid velocity is given as:

$$u(x,\ y\to\infty)=U \tag{8}$$

The far field fluid temperature is maintained at a constant temperature at all times:

$$T(x,\ y\to\infty,\ t)=T_\infty \tag{9}$$

The surface temperature is initially a constant, T_{si}. The first order fluid temperature at the surface is written as:

$$T(x,\ y=0\,,\ t<0)=T_{si}+\frac{2-\sigma_T}{\sigma_T}\frac{2\gamma}{\gamma+1}\frac{\lambda}{\mathrm{Pr}}\frac{\partial T}{\partial y}(x,\ y=0\,,\ t<0) \tag{10}$$

The surface temperature is suddenly changed to T_{sf} at ($t = 0$) and is maintained constant. Hence, the temperature jump condition at the surface for $t \geq 0$ is:

$$T(x, y=0\,,\ t\geq 0)=T_{sf}+\frac{2-\sigma_T}{\sigma_T}\frac{2\gamma}{\gamma+1}\frac{\lambda}{\mathrm{Pr}}\frac{\partial T}{\partial y}(x,\ y=0\,,\ t\geq 0) \tag{11}$$

where σ_T is the thermal accommodation coefficient, γ is the specific heat ratio, and Pr is the Prandtl number. The first-order conditions given in Eqs. (6), (10), (11) are applicable to the slip flow regime where the Knudsen number is in the range 0.001 ~ 0.1. In the transition regime where the Knudsen number is between 0.1 ~ 10, the continuum assumption breaks, and higher order slip conditions are required [1]. Detailed discussion on the origin of the slip conditions (Eqs. (6), (10), (11), the accommodation coefficients as well as their experimental values can be found in [18] and [19].

The solution of this problem is carried out in this work using similarity transformation. From inviscid flow solution, the velocity outside the boundary layer is given as:

$$U=B\,x \tag{12}$$

where B is an arbitrary constant with a dimension of (t^{-1}).

Defining the stream function ψ and the dimensionless variable η as:

$$\psi(x,\ y)=x^{n-1}\sqrt{B\nu}\ F(\eta) \tag{13}$$

$$\eta(x,\ y)=y\sqrt{B/\nu} \tag{14}$$

It follows directly from Eqs. (12) ~ (14) that:

$$u(x,\ y)=\frac{1}{x^{n-2}}\frac{\partial\psi}{\partial y}=U\,F'(\eta)=B\,x\,F'(\eta) \tag{15}$$

$$\upsilon=-\frac{1}{x^{n-2}}\frac{\partial\psi}{\partial x}=-(n-1)\sqrt{B\nu}F(\eta) \tag{16}$$

Using the following definition for the dimensionless temperature:

$$G(\eta,\ t)=\frac{T(x,\ y,\ t)-T_\infty}{T_\infty} \tag{17}$$

the momentum and energy equations are transformed into the following equations:

$$F'''+(n-1)FF''+1-F'^2=0 \tag{18}$$

$$\frac{B}{Pr}\frac{\partial^2 G}{\partial\eta^2}+(n-1)\,BF\frac{\partial G}{\partial\eta}=\frac{\partial G}{\partial t} \tag{19}$$

Using the following function for the dimensionless temperature:

$$\theta(\eta,\ \tau)=G(\eta,\ t) \tag{20}$$

where

$$\tau=\frac{U\,t}{x} \tag{21}$$

Equation (19) is transformed into the following partial differential equation:

$$\frac{\partial^2\theta}{\partial\eta^2}+(n-1)\,\mathrm{Pr}\,F\frac{\partial\theta}{\partial\eta}=\mathrm{Pr}\frac{\partial\theta}{\partial\tau} \tag{22}$$

The boundary and initial conditions (6) ~ (11) are transformed into the following forms:

$$F'(0)=K_V\,F''(0) \tag{23}$$

$$F(0)=0 \tag{24}$$

$$F'(\eta\to\infty)=1 \tag{25}$$

$$\theta(\eta=0,\ \tau<0)=\theta_{si}+K_T\frac{\partial\theta}{\partial\eta}(\eta=0,\ \tau<0) \tag{26}$$

$$\theta(\eta=0,\ \tau\geq 0)=\theta_{sf}+K_T\frac{\partial\theta}{\partial\eta}(\eta=0,\ \tau\geq 0) \tag{27}$$

$$\theta(\eta\to\infty,\ \tau)=0 \tag{28}$$

https://doi.org/10.1017/jmech.2014.33 Published online by Cambridge University Press

where θ_{si}, θ_{sf} are respectively the dimensionless surface temperatures at the initial and final states, defined as:

$$\theta_{si} = \frac{T_{si} - T_\infty}{T_\infty}, \quad \theta_{sf} = \frac{T_{sf} - T_\infty}{T_\infty} \tag{29}$$

and K_V, K_T are respectively, the velocity slip and temperature jump factors, given as:

$$K_V = \frac{2-\sigma_V}{\sigma_V}\lambda\sqrt{B/\nu} = \frac{2-\sigma_V}{\sigma_V}Kn \tag{30}$$

$$K_T = \frac{2-\sigma_T}{\sigma_T}\frac{2\gamma}{\gamma+1}\frac{\lambda}{\mathrm{Pr}}\sqrt{B/\nu} = \frac{2-\sigma_T}{\sigma_T}\frac{2\gamma}{\gamma+1}\frac{1}{\mathrm{Pr}}Kn \tag{31}$$

Noting that the term $\sqrt{B/\nu}$ in Eqs. (30), (31) has the dimension of (L^{-1}), the characteristic length of the flow may be taken as $L_c = \sqrt{\nu/B}$, and the Knudsen number Kn in Eqs. (30), (31) is defined accordingly:

$$Kn = \frac{\lambda}{\sqrt{\nu/B}} \tag{32}$$

when the final steady state is reached, the right-hand side of Eq. (22) approaches zero, and hence the steady energy equation is an ordinary differential equation of the form:

$$\theta'' + (n-1)\,\mathrm{Pr}\,F\,\theta' = 0 \tag{33}$$

The boundary condition for Eq. (33) at $\eta \to \infty$ is the same as given in Eq. (28), and at the surface, the boundary conditions given by Eqs. (26) and (27) become:

$$\theta(\eta = 0) = \theta_{si} + K_T\,\theta'(\eta = 0), \text{ at the initial steady state} \tag{34}$$

$$\theta(\eta = 0) = \theta_{sf} + K_T\,\theta'(\eta = 0), \text{ at the final steady state} \tag{35}$$

The Nusselt number may be found from Newton's law of cooling and Fourier's law of heat conduction at the surface:

$$h\,(T_s - T_\infty) = -k\left.\frac{\partial T}{\partial y}\right|_{y=0} \tag{36}$$

Using Eqs. (14), (17), (20) in Eq. (36), the following expression for Nusselt number is obtained:

$$Nu_x.Re_x^{-1/2} = -\theta'(0)/\theta_s \tag{37}$$

An implication of the no velocity slip condition at the surface is that a very thin layer of the fluid is formed at the surface where heat transfer is by pure conduction. The heat conducted through this stagnant layer is then convected through the fluid, so that with no velocity slip, one arrives at the formal definition of the convective heat transfer coefficient by equating the above two expressions.

With a non-zero velocity slip, where the fluid at the surface has a finite non-zero velocity, the heat transfer at the surface is no longer pure conduction. The shear work at the boundary (work done by the fluid on the surface) [22-24] due to the slipping fluid is not accounted for in calculating the heat flux at the surface. It was shown [25] that the shear work at the boundary is dependent on the viscous dissipation and the degree of rarefaction, so that with the assumption of negligible viscous dissipation in this work, the above expression for the Nusselt number is valid.

The slip parameters K_V and K_T are constants (independent of the position along the surface) as is clear from Eqs. (30), (31). Therefore the self-similarity of stagnation point flow is preserved. As explained in references [4], [7] and [8], the self-similar transformation for other flow geometries (*e.g.*, flow over a flat plate, or a wedge), the self-similarity is lost due to slip conditions at the wall, where the slip parameter is no longer a constant. Since the parameters K_V, K_T are functions of the surface conditions and the Knudsen number, the results are presented in terms of these parameters rather than the Knudsen number, so as to cover a wide range of surface conditions, keeping in mind that the model presented in this work is valid within the slip flow regime (*i.e.*, $Kn \le 0.1$). All the results shown are for Prandtl number of Pr = 0.71 unless otherwise stated.

3. NUMERICAL SOLUTION METHOD AND VERIFICATION

Equations (18), (22) are analyzed numerically to study the effect of velocity slip and temperature jump conditions on the thermal boundary layer response when the surface is exposed to sudden heating and cooling processes. The initial- and final-steady state solutions are first obtained by solving the governing equation of the hydrodynamic problem together with the steady energy equation (*i.e.*, Eqs. (18), (33). The DBVPFD subroutine of the IMSL library is used to integrate these equations subject to the conditions given by Eqs. (23) ~ (25), (28), (34) for the initial steady solution, and the conditions given by Eqs. (23) ~ (25), (28), (35) to obtain the final steady state solution. The DBVPFD subroutine uses variable step size finite difference method with deferred corrections.

The unsteady energy equation (Eq. (22)) subject to the conditions given by Eqs. (26) ~ (28) is solved by an implicit finite difference method. Central difference formulas accurate to $O(\Delta\eta^2)$ are used for the spatial derivatives and a backward difference formula of $O(\Delta\tau)$ accuracy is used for the temporal derivative. The resulting diagonally-dominant tri-diagonal system of equations is solved using a direct solver with the Thomas algorithm.

For $K_V = 0$, it was found that $F'(\eta_\infty) \ge 0.999$ at $\eta_\infty \ge 3.140$ for planar flow and at $\eta_\infty \ge 2.496$ for axisymmetric flow. For Pr = 0.5 with $K_V = K_T = 0$, it was found that $\theta(\eta_\infty) \le 0.001$ at $\eta_\infty \ge 5.132$ in planar flow, and at $\eta_\infty \ge 4.358$ in axisymmetric flow [20]. The computa-

https://doi.org/10.1017/jmech.2014.33 Published online by Cambridge University Press

tional domain in this work is extended to $\eta_\infty \geq 5.2$ for computations with Pr = 0.71, to ensure that the calculations are extended beyond both the velocity and thermal boundary layers.

The grid size chosen is $\Delta\eta = 2.0 \times 10^{-3}$ and the time step is taken as $\Delta\tau = 1 \times 10^{-4}$. Grid sensitivity analysis is performed to ensure the solutions obtained are grid independent. The accuracy of the numerical solution obtained is verified by comparing the results at large times with steady state solutions of the problem, and with results available in literature. To ensure the highest level of accuracy, the tolerance used in the DBVPFD subroutines is set to 10^{-9}. The steady solution of the transient energy equation is assumed to be reached at time $\tau = \tau_{ss}$ where the maximum relative percentage difference between the solution of the unsteady energy equation (Eq. (22)) and that of the steady energy equation (Eq. (33)) in the whole domain is less than 1%, *i.e.*,

$$\left|\frac{\theta_n(\eta,\tau)-\theta_e(\eta,\tau)}{\theta_e(\eta,\tau)}\right|_{\max} < 0.01 \qquad (38)$$

where $\theta_n(\eta, \tau)$ is the solution of Eq. (22) and $\theta_e(\eta, \tau)$ is the solution of Eq. (33).

The accuracy of the results presented in this work is verified using different measures. Table 1 shows a comparison between the present solutions and those reported in [26] of the dimensionless velocity gradient at the surface $[F''(0)]$ (a measure of the shear stress) over a range of velocity-slip factor, $0 \leq K_V \leq 50$. The numerical solution of the hydrodynamic problem (Eq. (18)) clearly compares very well with those reported in [26] for all the velocity-slip factors chosen in both the planar and axisymmetric flow settings.

Table 2 shows a comparison between the present solutions and those reported in [26] of the dimensionless temperature gradient at the surface $[-\theta'(0)]$ (a measure of the heat transfer rate) for different values of velocity-slip and temperature-jump factors, which are set as equal (*i.e.*, $K_T = K_V$) for convenience of calculations, as the values of $F''(0)$ are tabulated in [26] for different values of K_V as shown in Table 1. The solution for the axisymmetric flow case ($n = 3$) of $[-\theta'(0)]$ reported in [26] is valid for any values of K_T and K_V, while that for planar flow is valid only for large values of K_V. Hence the comparison for the latter case between the present solution and that in [26] is shown only for $K_V \geq 10$. The solution of the transient energy Eq. (22) shown in Table 2 corresponds to a sudden cooling process with $\theta_{si} = 2.0$, $\theta_{sf} = 1.0$. The solution of the steady state energy Eq. (33) compares very well with that of the unsteady energy Eq. (22) at the final steady state (*i.e.*, at $\tau = \tau_{ss}$) with a percentage relative error of less than 1%, and they both compare very well with the results reported in [26].

4. RESULTS AND DISCUSSION

The effects of both the velocity slip and temperature jump factors on the thermal boundary layer response,

Table 1 Alues of $F''(0)$: A Comparison between present work and Ref. [26]

K_V	$n = 2$		$n = 3$	
	Ref. [26]	Solution of Eq. (18)	Ref. [26]	Solution of Eq. (18)
0.0	1.23259	1.232587	1.311938	1.311938
0.5	0.82148	0.821479	0.86688	0.866879
1.0	0.59346	0.593462	0.61730	0.617300
10.0	0.094036	0.094036	0.094597	0.094597
20.0	0.048472	0.048472	0.048620	0.048620
50.0	0.019752	0.019752	0.019776	0.019776

Table 2 Values of $[-\theta'(0)]$: A Comparison between present work and Ref. [26] for Pr = 1

K_T (= K_V)	$n = 2$				$n = 3$			
	Ref. [26]	Solution of Eq. (33)	Solution of Eq. (22) at τ_{ss}	τ_{ss}	Ref. [26]	Solution of Eq.(33)	Solution of Eq. (22) at τ_{ss}	τ_{ss}
0.0		0.570465	0.565760	2.961	0.76223	0.762231	0.755732	1.595
0.5		0.502826	0.499011	3.098	0.63799	0.637993	0.633355	1.679
1.0		0.416181	0.413554	3.275	0.50066	0.500664	0.497900	1.768
10.0	0.088863	0.088712	0.088608	3.691	0.091745	0.091745	0.091667	2.020
20.0	0.047051	0.047030	0.047002	4.051	0.047863	0.047863	0.047842	2.047
50.0	0.019511	0.019509	0.019505	4.110	0.020000	0.019651	0.019647	2.064

https://doi.org/10.1017/jmech.2014.33 Published online by Cambridge University Press

heat transfer and the time it takes to reach steady state conditions from a given initial steady state when the surface is suddenly heated or cooled are quantified numerically in this work. Table 2 shows the transition time and the temperature gradient of the fluid at the surface at the final steady state, when the surface is suddenly cooled from an initial temperature of $\theta_{si} = 2.0$ to a final temperature of $\theta_{sf} = 1.0$ for different values of temperature jump and velocity slip factors. For the same flow conditions, the transition time is clearly lower while the temperature gradient is higher in axisymmetric flow than in planar flow. This will be explained in this section. Moreover, the transition time τ_{ss} increases while the temperature gradient decreases with increasing the temperature jump in both axisymmetric and planar flow. However, since K_T and K_V are set equal in these computations, it is not clear from Table 2 how these factors affect the transition time and the heat transfer rate individually, and which factor has the prominent effect on the transition time, heat transfer rate and thermal boundary layer response to sudden surface conditions. The individual effects of these two factors on the transition time and heat transfer rate are detailed in this section in addition to a comparison between planar and axisymmetric flow settings in terms of thermal boundary layer response, heat transfer and transition time for surface sudden cooling and heating processes.

Velocity-slip effect on the time evolution of the temperature distribution in a sudden surface cooling process with $\theta_{si} = 2.0$ and $\theta_{sf} = 1.0$ is presented in Fig. 2. As a further check on the accuracy of the numerical solutions, the final steady state solution in Fig. 2 and in all of the results presented in this section are found by solving both the steady and unsteady energy equations (Eqs. (22), (33) and the two solutions coincide with no noticeable difference. With zero temperature-jump, the fluid is in thermal equilibrium with the surface and the fluid temperature at the surface, $\theta(0)$ remains constant. The temperature profiles exhibit a maximum value at some point in the domain that persists until $\tau \approx 0.2$ where heat is transferred from the fluid towards the surface in one portion of the domain, and towards the far-field fluid in the other portion. The effect of increasing the velocity slip tends to reduce the thermal boundary layer thickness and decrease the transition time. Moreover, most of the changes of the temperature during transition from the initial- to the final-steady state take place during the very first portion of the transition time. The increase in the velocity-slip results in a steeper temperature profile, hence an increase in the temperature gradient (in absolute sense) at the surface. This observation is made more clear in Fig. 3, showing the evolution in time of the temperature and temperature gradient at the surface for different values of velocity slip factor with $K_T = 1$, as well as in Fig. 4 that presents the spatial temperature gradient profiles at the initial- and final-steady states together with the transition time for four different values of velocity- slip with no temperature-jump. It can be concluded from Figs. 2 ~ 4 that higher velocity slip results in lower thermal boundary layer thickness, higher

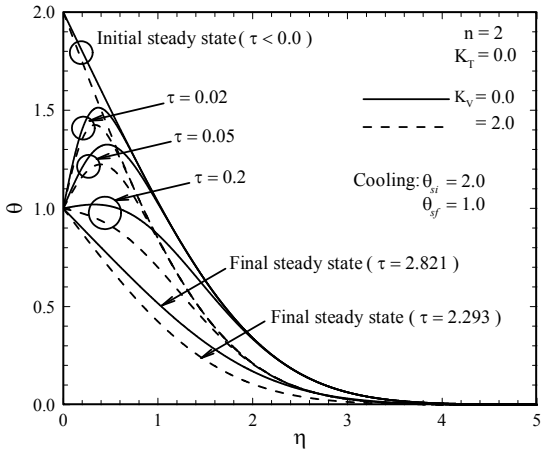


Fig. 2 Spatial temperature profiles at different times during transition in sudden surface cooling: Velocity slip effect with zero temperature jump

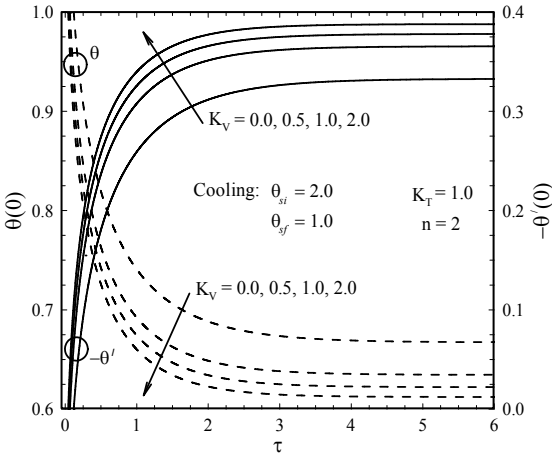


Fig. 3 Temporal evolution of the temperature and temperature gradient in the fluid at the surface during sudden cooling for different values of velocity slip with temperature jump

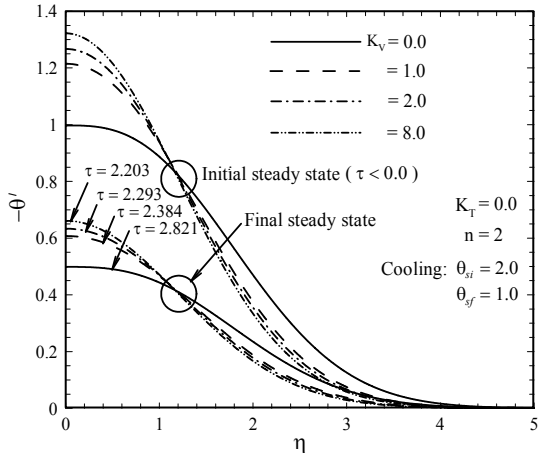


Fig. 4 Spatial temperature-gradient profiles at the initial and final steady states for different values of velocity slip with zero temperature jump in sudden cooling

https://doi.org/10.1017/jmech.2014.33 Published online by Cambridge University Press

temperature gradient at the surface and lower transition time. Velocity slip reduces the difference between the fluid velocity at the surface and that at the far-field, causing the velocity boundary layer thickness to decrease. Since the velocity and thermal boundary layer thicknesses are related by the Prandtl number, the reduction in the velocity boundary layer thickness results in a reduction of the thermal boundary layer thickness. Moreover, the velocity slip has the most profound effect on the temperature gradient (Figs. 3, 4), and hence on heat transfer rate, at low values of velocity slip (around $K_V \leq 3$) and the temperature gradient becomes less sensitive to variations in K_V as K_V increases.

Next, the effect of temperature-jump on transition time and thermal boundary layer response to sudden surface cooling is studied and the results are presented in Figs. 5 ~ 7. With a temperature jump of $K_T = 1.0$ (Fig. 5), the initial fluid temperature at the surface corresponding to the initial surface temperature $\theta_{si} = 2.0$ is $\theta(0) \approx 1.334$. The fluid temperature at the surface continues to change with time until the final steady state with $\theta(0) \approx 0.667$ is reached. Most of the changes in temperature (≈ 80%) take place during the very first portion (≈ 20%) of the transition time as also noticed in Fig. 2. Figures 6, 7 show respectively the temperature and temperature gradient distributions at the initial and final steady states for three different values of temperature jump and zero velocity slip. Higher temperature jump results in lower temperature gradient at the surface and higher transition time. It can be concluded from the results in Figs. 2 ~ 4 and 5 ~ 7, that temperature jump and velocity slip have opposite effects on the transition time and the temperature gradient in the fluid at the surface.

The temperature distribution at different times during transition in a sudden heating with $\theta_{si} = 1.0$, $\theta_{sf} = 2.0$ is shown in Fig. 8. The time evolution of the temperature gradient in the fluid at the surface is presented in Fig. 9, with zero temperature jump and a range of velocity-slip factor. As in the cooling case, the effect of increasing the velocity slip tends to thin the thermal boundary layer, increase the temperature gradient at the surface and decrease the transition time. The heat transfer in sudden heating is however maintained in one direction from the surface towards the far-field fluid during the whole transition period. A comparison between Figs. 2 and 8 shows that for the same conditions, even though the heating and cooling extents ($|\theta_{sf} - \theta_{si}|$) are equal, the transition time is less in heating than in cooling. This is due to the fact that the transition time is inversely proportional to the final temperature gradient of the fluid at the surface, which is higher in heating than in cooling for these two cases. In other words, for the same heating/cooling extent, the transition time is less when the process is towards higher temperature gradient (in absolute sense) at the surface. This is also made clear through a comparison between Figs. 10, 11 (heating) with Figs. 4, 7 (cooling). It was shown in [20] that the transition time due to impulsive surface temperature changes with no slip effects is inversely proportional to the final temperature gradient at the surface [*i.e.*, $\tau_{ss} \propto 1/\theta'(0)$]. This relation

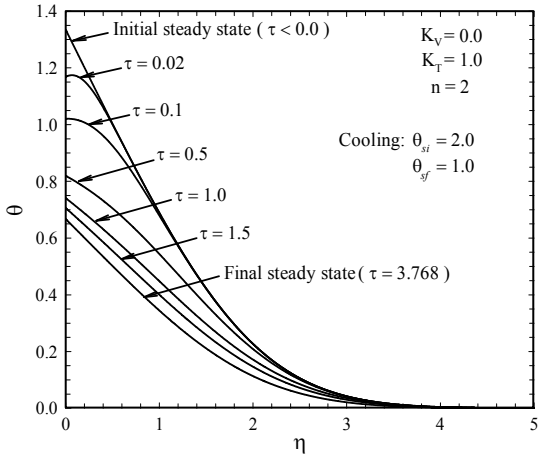


Fig. 5 Spatial temperature profiles at different times during transition in sudden surface cooling: Temperature jump effect with zero velocity slip

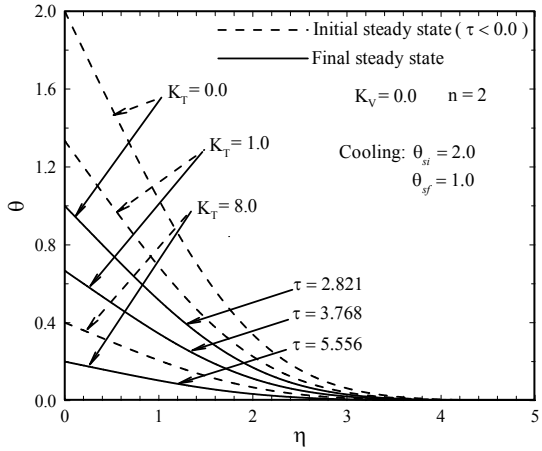


Fig. 6 Spatial temperature profiles at the initial and final steady states for different values of temperature jump with zero velocity slip

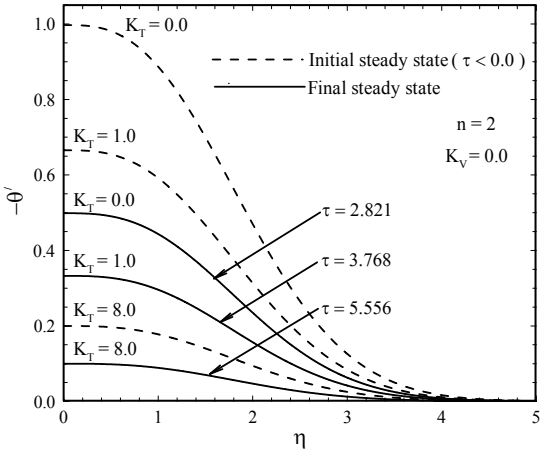


Fig. 7 Spatial temperature-gradient profiles at the initial and final steady states for different values of temperature jump with zero velocity slip in sudden cooling

https://doi.org/10.1017/jmech.2014.33 Published online by Cambridge University Press

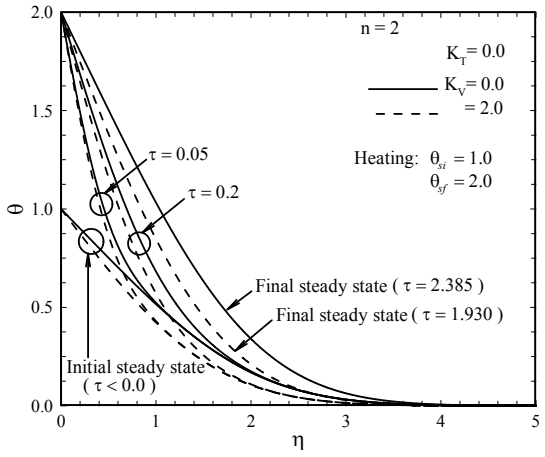


Fig. 8 Spatial temperature profiles at different times during transition in sudden surface heating: Velocity slip effect with zero temperature jump

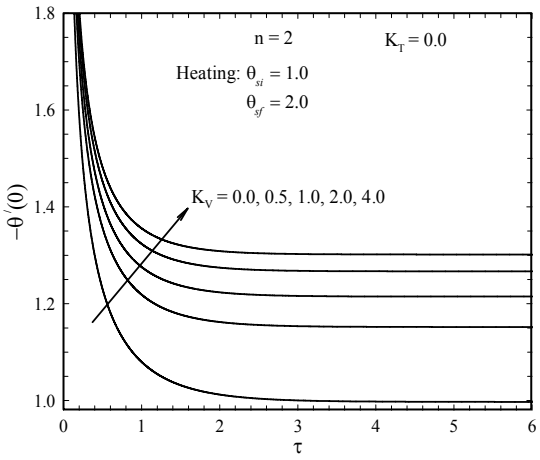


Fig. 9 Temporal evolution of the temperature gradient in the fluid at the surface during sudden heating for different values of velocity slip with zero temperature jump

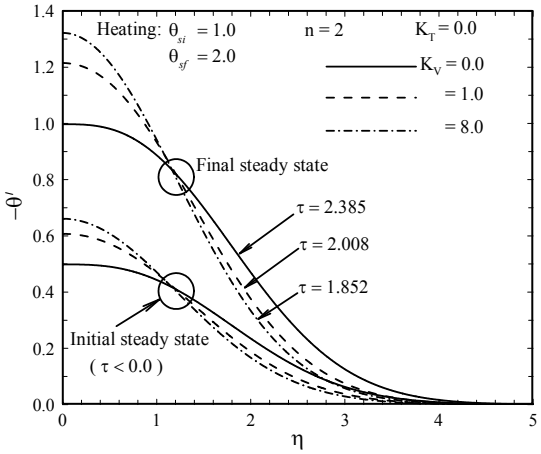


Fig. 10 Spatial temperature-gradient profiles at the initial and final steady states for different values of velocity slip with zero temperature jump in sudden heating

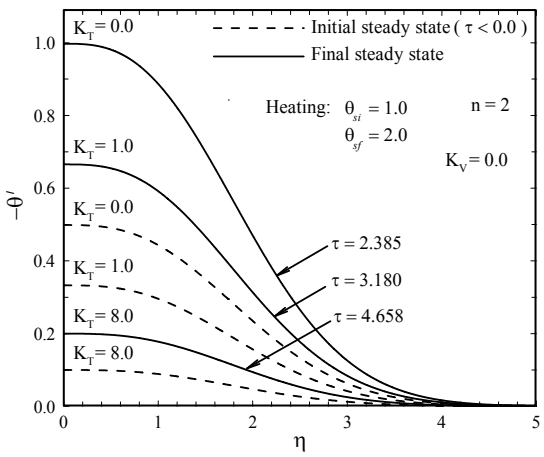


Fig. 11 Spatial temperature-gradient profiles at the initial and final steady states for different values of temperature jump with zero velocity slip in sudden heating

applies with slip effects as well, and it explains the relation between the transition time and the final temperature gradient at the surface when the surface conditions are suddenly changed. The total heat transferred per unit area during the transition time τ_{ss} can be written as:

$$Q'' = \int_0^{\tau_{ss}} \frac{x}{U} q_s''(\tau)\, d\tau \tag{39}$$

where q_s'', is the surface heat flux. This can be written as:

$$q_s'' \propto \left[\frac{\partial T}{\partial y}\Big|_{y=0} = -\sqrt{U / \nu x}\; T_\infty\, \theta'(0,\ \tau) \right] \tag{40}$$

Using (40) in (39):

$$Q'' \propto \int_0^{\tau_{ss}} \theta'(0,\ \tau)\, d\tau \tag{41}$$

Equation (41) may be written as:

$$Q'' \propto \bar{\theta}'(0).\tau_{ss} \tag{42}$$

where $\bar{\theta}'(0)$ is the average dimensionless temperature gradient at the surface during the transition time. The transition time is written as:

$$\tau_{ss} \propto \frac{Q''}{\bar{\theta}'(0)} \tag{43}$$

The transition time is clearly directly proportional to total heat transferred and inversely proportional to the heat transfer rate. As can be noticed from Figs. 2, 5, 8, most of the change in the temperature gradient at the surface occurs during the first small portion (20%) of the transition time. Hence, it is the slight change in the temperature gradient taking place afterwards that determines τ_{ss}. Therefore, the above relation can be written as:

https://doi.org/10.1017/jmech.2014.33 Published online by Cambridge University Press

$$\tau_{ss} \propto \frac{Q''}{\theta'(0)} \tag{44}$$

where $\theta'(0)$ is the final temperature gradient of the fluid at the surface.

The relations between the transition time and the momentum and thermal discontinuities in surface sudden cooling and heating processes are shown in Figs. 12 ~ 15 for planar and axisymmetric flows in both cooling and heating processes. Figures 12, 13 show that in both cooling and heating processes, increasing the velocity slip decreases the transition time and that the velocity slip is most influential on the transition time at relatively low values of velocity slip ($K_V \leq 3$). Also, the transition time increases with increasing the temperature jump. Moreover, the transition time is less in axisymmetric than in planar flow, which is due to the fact that the thermal boundary layer thickness is less in axisymmetric flow than in planar flow, resulting in higher temperature gradients at the surface. Using scaling analysis of the governing equations, it can be shown [20] that the transition time scales with $1/(n-1)$, *i.e.*, $\tau_{ss} \sim 1/(n-1)$. The effect of increasing the velocity slip in both cooling and heating is to increase the temperature gradient at the surface and decrease the thermal boundary layer thickness resulting in a decrease in the transition time. The effect of increasing the temperature jump in both cooling and heating is to reduce the temperature gradient at the surface leading to an increase in the transition time, and to reduce the thermal boundary layer thickness, leading to a decrease in the transition time. With these two opposing factors on the transition time, Figs. 14, 15 clearly show that the effect of the temperature gradient dominates, resulting in an increase in the transition time.

Figures 16 and 17 demonstrate the relation between the Nusselt number and the velocity slip and temperature jump respectively, in both axisymmetric and planar settings at steady state conditions.

As shown in Fig. 16, the Nusselt number increases with increasing the velocity slip and so does the heat transfer rate. Figure 17 shows that the Nusselt number decreases with increasing the temperature jump. The velocity slip and temperature jump clearly have opposite effects on the rate of heat transfer. This is explained by the fact that the temperature gradient at the surface increases with the velocity slip (as shown in Figs. 3, 4, 9, 10) leading to an increase in heat transfer rate, while higher temperature jump leads to lower temperature gradient (Figs. 6, 8, 11), and hence lower heat transfer rate.

5. CONCLUSIONS

Transient convection in laminar incompressible stagnation point flow with velocity slip and temperature jump is studied numerically in this work. The individual effects of the velocity slip and temperature jump on the thermal boundary layer response, heat transfer and transition time are analyzed for impulsive changes

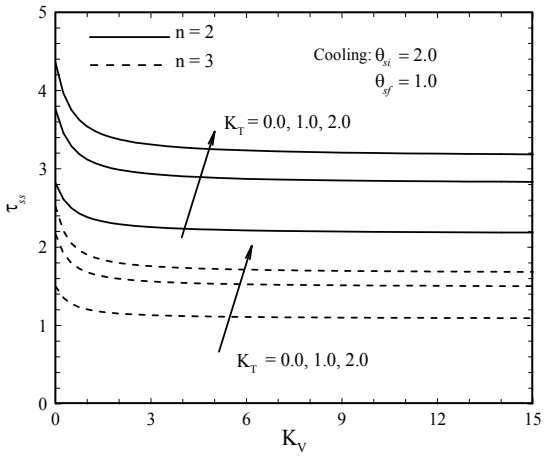


Fig. 12 Variation of transition time with temperature jump factor at different values of velocity slip factor for both planar and axisymmetric flow configurations with sudden surface cooling

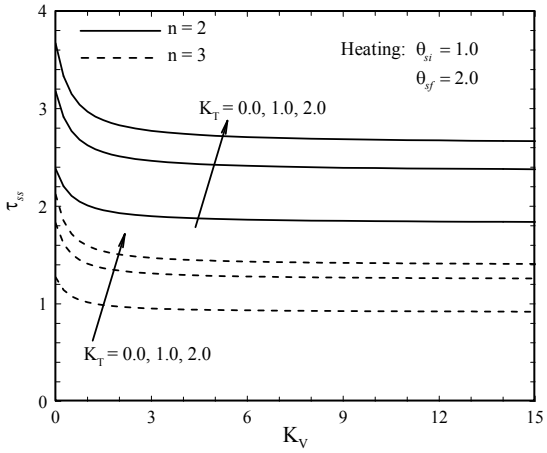


Fig. 13 Variation of transition time with velocity slip factor at different values of temperature jump for both planar and axisymmetric flow configurations with sudden surface heating

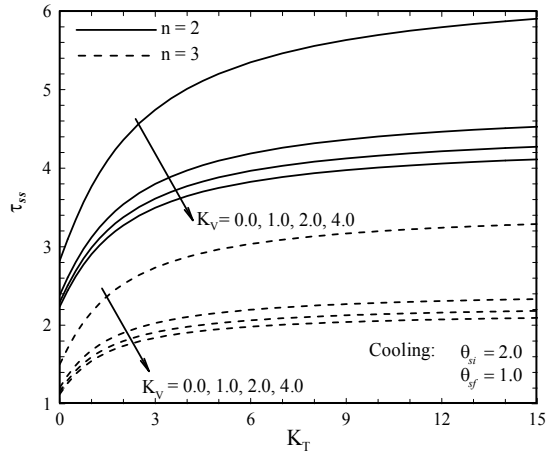


Fig. 14 Variation of transition time with temperature jump factor at different values of velocity slip factor for both planar and axisymmetric flow configurations with sudden surface cooling

https://doi.org/10.1017/jmech.2014.33 Published online by Cambridge University Press

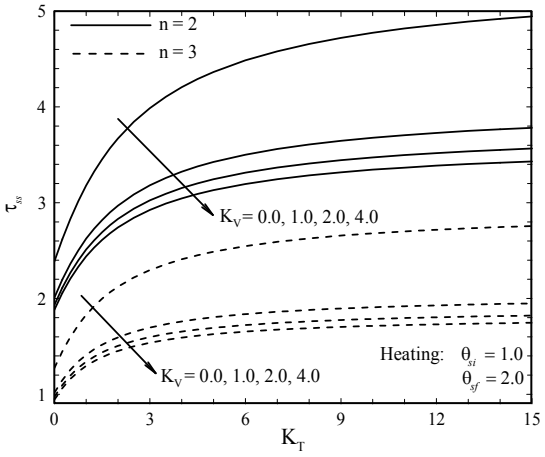


Fig. 15 Variation of transition time with temperature jump factor at different values of velocity slip factor for both planar and axisymmetric flow configurations with sudden surface heating

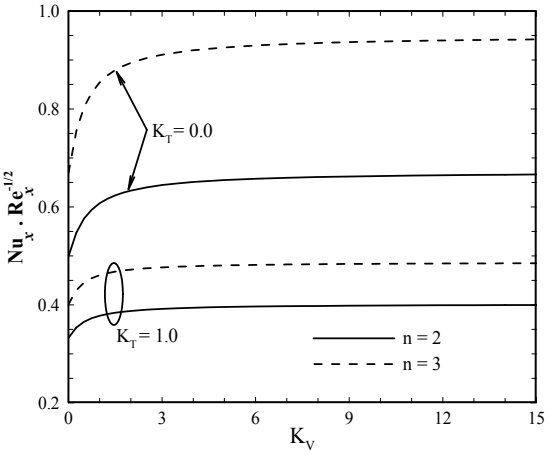


Fig. 16 Relation at steady state conditions between the velocity slip and Nusselt number for axisymmetric and planar flow

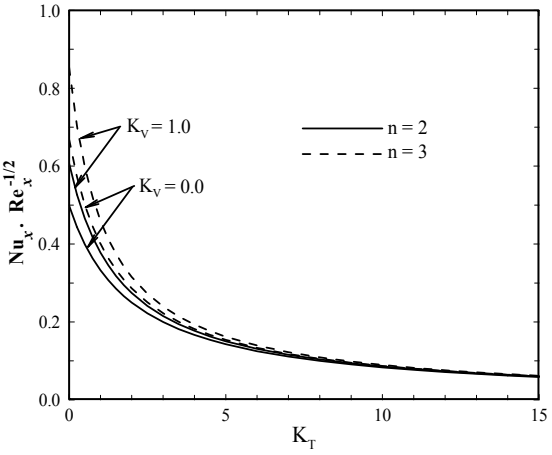


Fig. 17 Relation at steady state conditions between the temperature jump and Nusselt number for axisymmetric and planar flow

in the surface temperature in both planar and axisymmetric flow configurations. It is found that an increase in the velocity slip enhances heat transfer, reduces the thermal boundary layer thickness and decreases the transition time. The velocity slip has the most profound effect on the transition time, heat transfer rate and thermal boundary layer thickness at low values of velocity slip and these parameters become less sensitive to variations in the velocity slip as the velocity slip increases. An increase in the temperature jump reduces the thermal boundary layer thickness, increases the transition time and decreases the heat transfer rate. The effect of increasing the temperature jump in both cooling and heating is to reduce the temperature gradient at the surface leading to an increase in the transition time, a reduction the thermal boundary layer thickness and a decrease in the transition time. With these two opposing factors on the transition time, the effect of the temperature gradient dominates, resulting in an increase in the transition time. The transition time when the surface is exposed to a sudden temperature change is strongly dependent on the value of the temperature gradient at the final steady state, so that for the same cooling/heating extent, the transition time is less when the process is towards higher temperature gradient at the surface.

NOMENCLATURES

A	Heat transfer area.
F	Similarity dimensionless stream function.
G	Dimensionless temperature as a function of the actual time, $G = [T - T_\infty]/T_\infty$.
h	Convective heat transfer coefficient.
K_V	Velocity slip factor.
K_T	Temperature jump factor.
L	Characteristic length.
Pr	Prandtl number, Pr = ν/α.
q''	Heat flux.
Q''	Total heat transferred per unit area.
Nu_x	Nusselt number, $Nu_x = hx/k$.
Re_x	Reynolds number based on the length x, $\mathrm{Re}_x = Ux/\nu$.
t	Time.
T	Temperature.
$T(0)$	Dimensional temperature of the fluid at the surface.
T_{si}	Initial dimensional temperature of the surface (at $\tau < 0$).
T_{sf}	Final dimensional temperature of the surface (at $\tau \geq 0$).
u	Velocity component in the x- direction.
U	Free stream velocity.
υ	Velocity component in the y- direction.
x, y	Coordinates.

Greek symbols

η	Similarity variable, $\eta = y\sqrt{B/\nu}$
τ	Dimensionless time, $\tau = U\,t\,/\,x$

https://doi.org/10.1017/jmech.2014.33 Published online by Cambridge University Press

τ_{ss} Dimensionless transition time from the initial- to the final- steady state
θ Dimensionless temperature as a function of the dimensionless time, $\theta(\eta, \tau) = G(\eta, t)$
θ_s Dimensionless temperature of the surface
θ_{si} Initial dimensionless temperature of the surface (at $\tau < 0$)
θ_{sf} Final dimensionless temperature of the surface (at $\tau \geq 0$)
$\theta'(0)$ Temperature gradient at the surface
$\overline{\theta}'(0)$ Time-average temperature gradient at the surface
ψ Stream function, $\psi = x^{n-1}\sqrt{B\nu}\, F(\eta)$
λ Fluid mean free path
μ Dynamic viscosity
α Thermal diffusivity
γ Specific heat ratio
ρ Density
σ_T Thermal accommodation coefficient
σ_V Momentum accommodation coefficient
ν Kinematic viscosity

Subscripts

∞ Free stream conditions
s Surface
ss Steady state
i Initial state
f Final state

REFERENCES

1. Gad-el-Hak, M., "The Fluid Mechanics of Microdevices – The Freeman Scholar Lecture," *Journal of Fluids Engineering*, ASME, **121**, pp. 5–33 (1999).
2. Mueller, T. J. and DeLaurier, J. D., "Aerodynamics of Small Vehicles," *Annual Review of Fluid Mechanics*, **35**, pp. 89–111 (2003).
3. Sun, Q., Boyd, I. D. and Candler, G. V., "Numerical Simulation of Gas Flow Over Microscale Airfoils," *Journal of Thermophysics and Heat Transfer*, **16**, pp. 171–179 (2002).
4. Martin, M. J. and Boyd, I. D., "Blasius Boundary Layer Solution with Slip Flow Conditions," Bartel, T. J. and Gallis, M. A. (Eds.), *22nd Rarefied Gas Dynamics Symposium*, Sydney, Australia (2000).
5. Vedantam, N. K., "Effects of Slip on Flow Characteristics of a Laminar Flat Plate Boundary Layer," *Proceedings of the ASME Fluids Engineering Summer Meeting*, Miami, FL, pp. 1551–1560 (2006).
6. Martin, M. J. and Boyd, I. D., "Stagnation-Point Heat Transfer Near the Continuum Limit," *AIAA Journal*, **47**, pp. 283–285 (2009).
7. Martin, M. J. and Boyd, I. D., "Momentum and Heat Transfer in a Laminar Boundary Layer with Slip Flow," *Journal of Thermophysics and Heat Transfer*, **20**, pp. 710–719 (2006).
8. Martin, M. J. and Boyd, I. D., "Falkner-Skan Flow over a Wedge with Slip Boundary Conditions," *Journal of Thermophysics and Heat Transfer*, **24**, pp. 263–270 (2010).
9. Aziz, A., "Hydrodynamic and Thermal Slip Flow Boundary Layers over a Flat Plate with Constant Heat Flux Boundary Condition," *Communications in Nonlinear Science and Numerical Simulation*, **15**, pp. 573–580 (2010).
10. Castelloes, F. V., Cardoso, C. R., Couto, P. and Cotta, R. M., "Transient Analysis of Slip Flow and Heat Transfer in Microchannels," *Heat Transfer Engineering*, **28**, pp. 549–558 (2007).
11. Yang, J. and Kwok, D. Y., "Time dependent Laminar Electrokinetic Slip Flow in Infinitely Extended Rectangular Microchannels," *Journal of Chemical Physics*, **118**, pp. 354–363 (2003).
12. A. Bhattacharyya, A., Masliyah, J. H. and Yang, J., "Oscillating Laminar Electrokinetic Flow in Infinitely Extended Circular Microchannels," *Journal of Colloid and Interface Science*, **261**, pp. 12–20 (2003).
13. Wiwatanapataphee, B., Wu, Y. H. and Hu, M., "Chayantrakom, K., a Study of Transient Flows of Newtonian Fluids Through Micro-Annuals with a Slip Boundary," *Journal of Physics A: Mathematical and Theoretical*, **42**, 065206 (2009), doi:10.1088/1751-8113/42/6/065206.
14. Colin, S., "Rarefaction and Compressibility Effects on Steady and Transient Gas Flows in Microchannels," *Microfluidics and Nanofluidics*, **1**, pp. 268–279 (2005).
15. Bestman, A. R., Ikonwa, I. O. and Mbelegodu, I. U., "Transient Slip Flow," *International Journal of Energy Research*, **19**, pp. 275–277 (1995).
16. Mukhopadhyay, S., "Effects of Slip on Unsteady Mixed Convective Flow and Heat Transfer Past a Stretching Surface," *Chinese Physics Letters*, **27**, 124401 (2010).
17. Bhattacharyya, K., Mukhopadhyay, S. and Layek, G. C., "Slip Effects on an Unsteady Boundary Layer Stagnation-Point Flow and Heat Transfer towards a Stretching Sheet," *Chinese Physics Letters*, **28**, 094702 (2011).
18. Karniadakis, G., Beskok, A. and Aluru, N., *Microflows and Nanoflows, Fundamentals and Simulation*, Springer Science, New York (2005).
19. Sharipov, F., "Data on the Velocity Slip and Temperature Jump on a Gas-Solid Interface," *Journal of Physical and Chemical Reference Data*, **40**, 023101 (2011).
20. Ramadan, K. and Al-Nimr, M. A., "On Impulsively Started Convection: The Case of Stagnation Point Flow," *International Journal of Thermal Sciences*, **50**, pp. 2355–2364 (2011).
21. White, F. M., *Viscous Fluid Flow*, McGraw-Hill, New York (1974).
22. Colin, S., "Gas Microflows in the Slip Flow Regime: A Critical Review on Convective Heat Transfer," *Journal of Heat Transfer*, ASME, **134**, 020908

https://doi.org/10.1017/jmech.2014.33 Published online by Cambridge University Press

(2012).
23. Hong, C. and Asako, Y., "Some Considerations on Thermal Boundary Layer Condition of Slip Flow," *International Journal of Heat and Mass Transfer*, **53**, pp. 3075–3079 (2010).
24. Hong, C., Y. Asako, Y. and Lee, J-H., "Heat Transfer Characteristics of Gaseous Flows in Micro-Channel with Constant Heat Flux," *International Journal of Thermal Sciences*, **46**, pp. 1153–1162 (2007).
25. Hadjiconstantinou, N. G., "Dissipation in Small Scale Gaseous Flows," *Journal of Heat Transfer*, ASME, **125**, pp. 944–947 (2003).
26. Wang, C. Y., "Stagnation Slip Flow and Heat Transfer on a Moving Plate," *Chemical Engineering Science*, **61**, pp. 7668–7672 (2006).

(Manuscript received October 19, 2013,
accepted for publication January 19, 2014.)

https://doi.org/10.1017/jmech.2014.33 Published online by Cambridge University Press